Weak antilocalization and linear magnetoresistance in the surface state of SmB_{6}

S. Thomas, D. J. Kim, S. B. Chung, T. Grant, Z. Fisk, and Jing Xia

Phys. Rev. B **94**, 205114 — Published 9 November 2016

DOI: 10.1103/PhysRevB.94.205114

Weak Antilocalization and Linear Magnetoresistance in The Surface State of SmB_6

S. Thomas[1], D.J. Kim[1], S.B. Chung[2], T. Grant[1], Z. Fisk[1] and Jing Xia[1]
[1]*Dept. of Physics and Astronomy, University of California, Irvine, California 92697, USA*
[2]*Physics Department, Seoul National University, Seoul, Korea (151-747)*

The strongly correlated Kondo insulator SmB_6 is known for its peculiar low temperature residual conduction, which has recently been demonstrated to arise from a robust metallic surface, as predicted by the theory of topological Kondo insulator (TKI). Photoemission, quantum oscillation and magnetic doping experiments have provided evidence for the Dirac-like dispersion and topological protection. Questions arise as whether signatures of spin-momentum locking and electron interaction could be resolved in transport measurements. Here we report metallic conduction of surface down to mK temperatures. We observe in the surface the weak-antilocalization (WAL) effect at small perpendicular magnetic fields. At larger perpendicular magnetic fields, the surface exhibits an unusual linear magnetoresistance similar to those found in Bi-based topological insulators and in graphene.

With its heavy f-electron degree of freedom, Kondo insulator[1] SmB_6[2] behaves as a correlated metal at high temperatures. Below 40 K the bulk of SmB_6 becomes insulating with the opening of Kondo energy gap due to the hybridization between conduction electrons and the highly renormalized f-electrons. The theory[3] of topological Kondo insulator predicted the existence of a topologically protected surface state (TSS) within this Kondo gap, naturally explaining the mysterious resistance saturation below 4 K[1]. Recent transport measurements[4–6] have confirmed the low temperature surface conduction and the robustness of the surface state (SS). This SS has been demonstrated[7] to vanish with a small amount of magnetic impurity but survives larger amount of non-magnetic doping, which is consistent with a TSS protected by time-reversal symmetry. Recent high resolution ARPES[8–10] and quantum oscillation[11] experiments have provided tentative evidence for the Dirac dispersion of the surface carriers, as expected in a TSS. Furthermore, unlike usual topological SS, first principle calculations[12,13] have predicted three surface Dirac bands residing at Γ and X/Y points, which agrees with ARPES-measured surface electronic structure[8–10], although the anticipated spin-momentum locking[14,15] awaits spin-resolved measurements. In this paper we perform transport studies of the SmB_6 SS down to 20 mK, checking whether transport signatures are consistent with those of spin-momentum locking and electron interaction effects.

High quality SmB_6 crystals were grown using the aluminum flux method. The surfaces of these crystals were carefully etched using hydrochloric acid and then cleaned using solvents to remove possible oxide layer or aluminum residues. These crystals are then inspected using X-ray analysis to make sure SmB_6 is the only content. Samples used in the experiments were made from these crystals either by mechanical cleaving or polishing using polishing films containing diamond particles. The exposed surfaces are (100) or (101) planes. Gold and platinum wires are attached to the samples using micro spot welding for electric contacts. Low frequency transport measurements were carried out in dilution fridges using either standard low frequency (17 Hz) lock-in techniques with 50 nA excitation currents.

Extending our previous work[6], we have verified the existence of SS in SmB_6 samples down to 20mK with non-local transport and thickness dependent Hall effect measurements. In particular, Fig. 1a demonstrates the non-local measurement from sample S11 with both (100) and (101) surfaces. The local voltage V_{Local} is measured at voltage leads close to the current lead on the (101) surface. And the non-local voltage V_{NL} is measured at voltage leads placed on the (100) side surface at the corner of the sample. The crossover from high temperature bulk conduction to low temperature surface dominated conduction is seen clearly from the temperature dependence of voltage ratio V_{NL}/V_{Local}, which increase 4 orders of magnitude as temperature is lowered, and saturates below 4 K down to 20 mK (Fig. 1b). We note that V_{NL}/V_{Local} approaches a large value of 30, which indicates better conduction on the (101) surface than (100) surface. We found both longitudinal resistance R_{xx} and hall slope R_{xy}/B continue their saturation to 20 mK, indicating the metallic surface doesn't localize even at our lowest temperature. A typical example is shown in Fig. 1c for a bar shaped sample with exposed (100) surfaces.

Weak antilocalization (WAL)[16] is expected in a TSS due to spin-momentum locking[14,15], which causes destructive interference between time-reversed electron paths and lowers the sample resistance. We note that WAL is not a definite proof for a topological surface state. This effect will be destroyed by a time-reversal-symmetry-breaking magnetic field, giving rise to magneto-resistance dip around zero field. Indeed we observe clear WAL effect in SmB_6 Samples at low temperatures. Fig. 2a shows the WAL effect at 20 mK of a thin plate SmB_6 sample S12B with dimensions t=120 μm, w=1100 μm, and L=3300 μm. With magnetic field

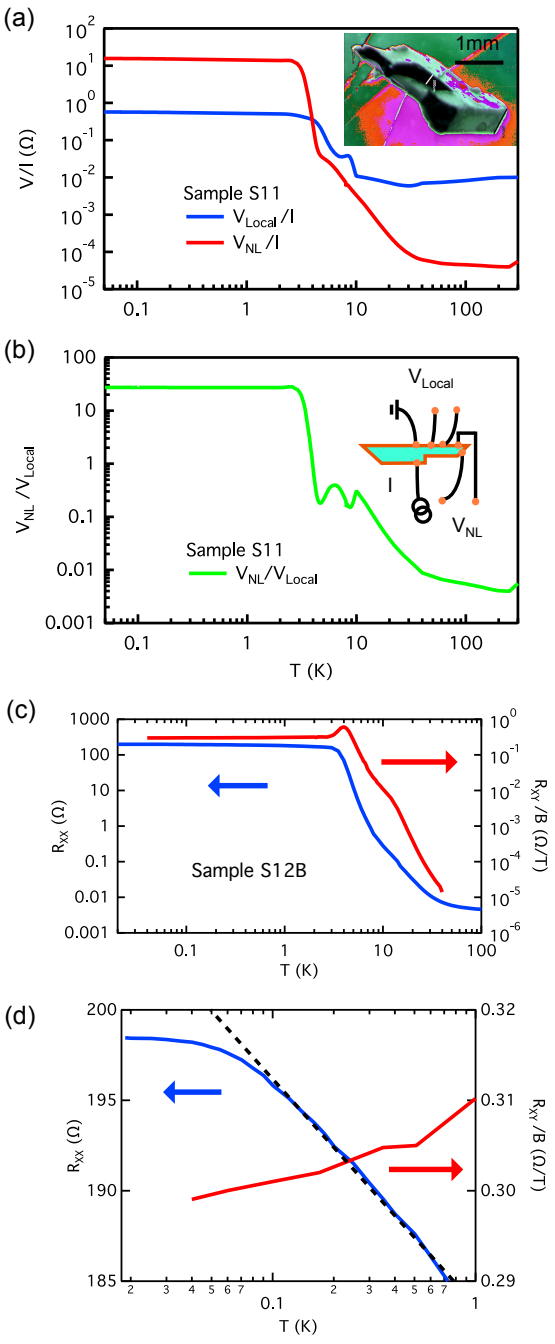

FIG. 1: **Surface conduction down to mK temperatures**. **(a)**, Temperature dependence of local and non-local resistance of an irregular thin-plate-shaped SmB_6 crystal S11 (inset). **(b)**, The ratio between non-local and local voltages increases 4 orders of magnitude as the temperature is lowered, and saturates below 3 K. This confirms the domination of surface conduction from 3 K down to 20 mK. Inset is a cross-sectional view of the sample with wiring schematics. **(c)**, Typical temperature dependence of R_{xx} and R_{xy}/B. **(d)**, Low temperature behaviors of R_{xx} and R_{xy}/B. R_{xx} displays logarithmic temperature dependence between 100 mK and 1 K and saturation below 100 mK, reminiscent of Kondo effect.

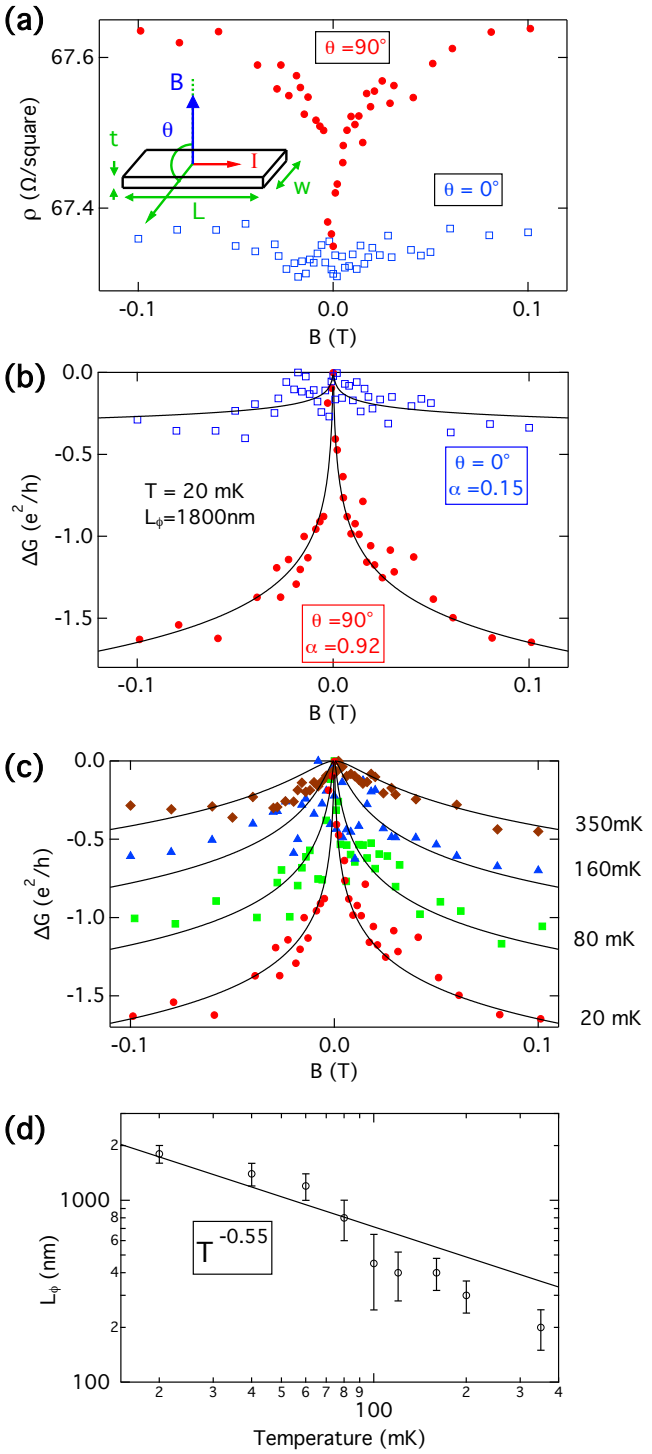

FIG. 2: **Weak antilocalization**. **(a)**, Magnetoresistance ρ at 20 mK of a thin plate sample S12B, with perpendicular (red dot) or in-plane (blue square) magnetic fields. Inset, orientation of magnetic field. **(b)**, $\Delta G = \Delta(1/\rho)$ fitted to Hikami-Larkin-Nagaoka (HLN) equation, yielding $\alpha = 0.92$. **(c)**, Temperature evolution of weak Antilocalization effect. Lines are fits using HLN equation with a fixed $\alpha = 0.92$ and variable dephasing length L_ϕ. **(d)**, L_ϕ at different temperatures, showing -0.55 power law behavior below 100 mK.

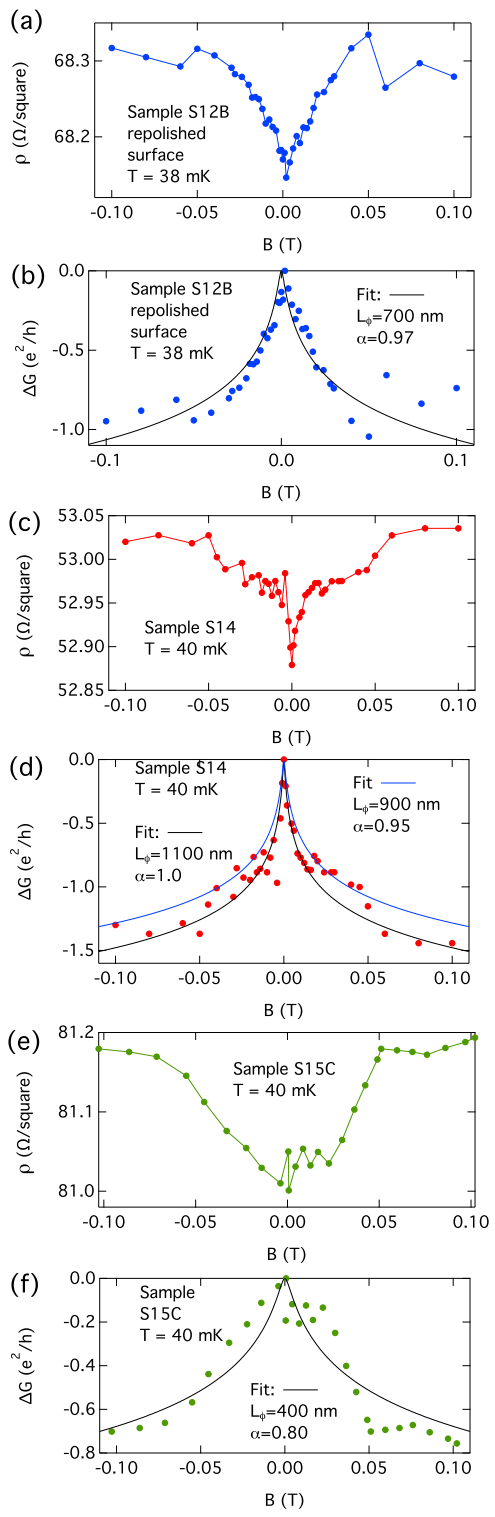

FIG. 3: **Weak antilocalization in other samples**. **(a),(b)**, Sample S12B after repolishing. Repolishing reduces the dephasing length L_ϕ to 700 nm at 38 mK. $\alpha = 0.97$ is however almost unchanged. **(c),(d)**, Sample S14, $L_\phi = 900nm$, $\alpha = 0.95$ at 40 mK. **(e),(f)**, Sample S15C, $L_\phi = 400nm$, $\alpha = 0.80$ at 40 mK.

perpendicular to the plate surface ($\theta = 90°$), a sharp resistivity dip occurs around zero field. The effect becomes almost invisible when the field is rotated to be perpendicular to the sidewall ($\theta = 0°$). This WAL signal is less clear in samples with large conductance. In the limit of long inelastic scattering time, WAL gives a negative quantum correction to the conductivity described by Hikami-Larkin-Nagaoka (HLN) equation[17]: $\Delta G = -\alpha[e^2/2\pi^2\hbar][ln(B_0/B) - \Psi(1/2 + B_0/B)]$, where $\Psi(x)$ is digamma function, B is perpendicular magnetic field component and $B_0 = \hbar/(4eL_\phi^2)$ with L_ϕ as dephasing length. Each independent conduction channel will contribute $\alpha = 1/2$. In Fig. 2b we fit the $\theta = 90°$ data to HLN equation and found $L_\phi = 1800nm$ and $\alpha = 0.92$. At $\theta = 0°$ the smaller side surfaces would contribute to WAL, but the fitted α parameter based on the conduction dominated by major surfaces will be seemingly smaller: : $\alpha' = \alpha t/w = 0.1$, which agrees reasonably with $\alpha' = 0.15$ that is fitted by fixing $L = 1800nm$. Weak antilocalization effect has been observed in several other samples as illustrated in Fig. 3, but we note that the signal of WAL effect is not observed in samples intentionally doped with the slightest amount of Gd and Ce magnetic impurities. Fitting them to HLN formula, we found that although the dephasing length L_ϕ varies a lot among samples, α values (0.8, 0.95 and 0.97) are rather close between samples, suggesting a universal value of 1. Taking into account both top and bottom surfaces, one might expect $\alpha = 3$ for a TI with three Dirac bands that have exactly the same L_ϕ. However, if one of the Dirac bands (e.g. Γ pocket) has a much larger L_ϕ than other bands, it will dominate WAL at small fields and make α appear to be 1. Alternatively, if inter-Dirac-band scattering become important compared to scatterings within an individual Dirac band, the three bands would behave effectively as a single channel as far as transport is concerned and will yield $\alpha = 1$. If indeed SmB_6 is a TKI with three Dirac bands[3,12,13,18], the $\alpha \approx 1$ value indicates either different dephasing lengths among surface bands or the importance of inter-band scattering. Fixing $\alpha = 0.92$ we could fit WAL data at different temperatures (Fig. 3c) and extract the temperature dependence of L_ϕ (Fig. 3d), which would be suggestive of dephasing mechanism. Below $T = 100\ mK$, L_ϕ scales as $T^{-0.55}$, which is different from the behavior above 100 mK. This is possibly related to the finite base electronic temperature of the Kondo physics discussed below. We note that our discussion here is based on the simplified HLN equation. Detailed discussions of these mechanisms are provided in a few recent theoretical publications including those in ref[27]. We have noticed a significant difference in L_ϕ of different samples (Fig. 3 a-f). A possible cause of this heterogeneity could be the different amount of residual magnetic impurities that would strongly affect L_ϕ at very low temperatures. With enough magnetic impurity, the surface state was found to be insulating with L_ϕ approaching zero[7].

The WAL effect would also result in a logarithmic de-

crease of resistance when temperature is lowered[16], a behavior that, like the WAL itself, would be quenched by a magnetic field. This however, is masked by the logarithmic resistance increase we observe from 1K to 100 mK (Fig. 1d) with the rate $dR_{xx}/d(\ln(T))$ almost independent of applied magnetic field (Fig. 4a). For two dimensional metals both interaction-induced Altshuler-Aronov (AA) effect[16] and the Kondo effect[19] could give rise to logarithmic resistance that survives large magnetic field. The AA effect gives a quantum correction to resistivity[16] $\Delta\rho = \rho^2 A\frac{e^2}{\pi h} ln(T_1/T_2)$ when the temperature changes from T_1 to T_2, where ρ is resistivity, $A \leq 1$ is a constant, e is electron charge and h is Plank's constant. From 1K to 100 mK, AA effect thus will increase the resistance R_{xx} in sample S12B by at most 0.3 Ω, which won't fully account for the observed 10 Ω increase (Fig. 1d). Furthermore, we found the relative changes of resistivity $\Delta\rho/\rho$ differ among samples by an order of magnitude, yet obey a very similar temperature dependence (Fig. 4b). This is hardly explained by AA correction alone, but is well described phenomenologically by Kondo effect. For spin 1/2 Kondo effect[20], the low temperature saturation resistivity is given by $\rho(T=0) = \rho_c + \rho_K$ and the resistivity in the logarithmic regime is given by $\rho(T) = \rho_c + \frac{\rho_K}{2}[1 - 0.47ln(1.2T/T_K)]$, where ρ_c and ρ_K represent the sizes of background and Kondo resistivities; T_K is the characteristic Kondo temperature. Using sample S12B, we could extract these three parameters by fitting in both the saturation and logarithmic regimes, yielding $T_K = 0.6K$. In Fig. 4b, we present the normalized resistance of 4 samples from different growth batches. Due to the similar temperature dependence, a universal $T_K = 0.6K$ seems to fit for all the samples. We could compare the normalized Kondo resistance $(\rho_{xx} - \rho_c)/\rho_K$ to the universal Kondo behavior calculated from numerical renormalization group calculations (NRG)[20]. As shown in Fig. 4c, from 20 mK to 1 K, the normalized Kondo resistance from different samples collapse to a single curve, which agrees well with NRG universal curve. The only exception is below 100 mK with sample S12D where both (100) and (101) surfaces exist on the measurement current path. In a perfect SmB_6 crystal, the Kondo effect from localized f-electrons and conduction electrons ceases to exist at low enough temperatures with the opening of the hybridization gap and due to coherent Kondo resonance[1]. However, when unavoidable trace amount of non-magnetic impurity substitutes Sm atoms near the surface, the resulting Kondo holes will give rise to the Kondo effect in the ungapped metallic surface state. Since T_K is determined by the strength of surface Kondo screening, a universal T_K is indeed expected, as we found experimentally. The relative size of resistivity change $\Delta\rho/\rho$, however, depends on several sample-specific factors including surface mobility and impurity concentration.

Metals with a closed Fermi surface and a principal charge carrier usually have positive magnetoresistance (MR) that is quadratic with magnetic field. In SmB_6

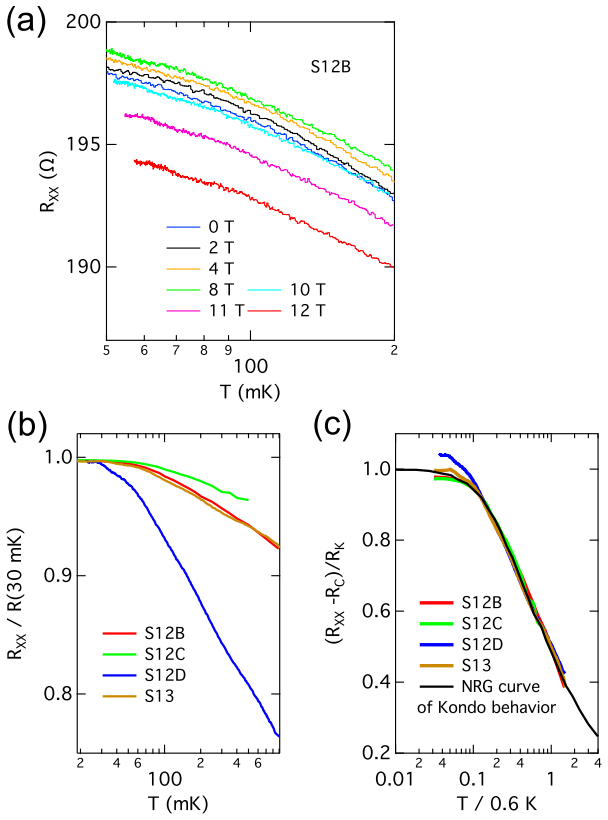

FIG. 4: **Surface Kondo effect**. **(a)**, R_{xx} vs T in sample S12B at various perpendicular fields. **(b)**, Temperature dependence of normalized resistance for various samples. **(c)**, Normalized resistance for various samples in comparison with universal numerical renormalization group (NRG) calculations.

at relative high temperatures when both bulk and surface conductions are important, the MR was found to be negative[21]. This is usually attributed to the magnetic-field-induced Zeeman energy competing with the spin scattering off the Kondo lattice, effectively reducing the Kondo gap[21]. Here we investigate surface magnetoresistance at mK temperatures when bulk conductions diminish. Orbital and Zeeman parts of the surface MR can be separately measured in thin plate samples by tilting the magnetic field perpendicular ($\theta = 90°$) and parallel ($\theta = 0°$) to the major surface: MR due to Zeeman effect shows up in both cases while only $\theta = 90°$ configuration will contain the orbital contribution. Fig. 5a summarizes the results from sample S12B. With in-plane field ($\theta = 0°$) at 40 mK the MR $\rho(\theta = 0°)$ due to Zeeman effect is negative and close to quadratic. Little difference was found whether the magnetic field is along or perpendicular to the current direction, confirming the Zeeman nature of in-plane MR. We note such a negative Zeeman contribution to the MR is consistent with the picture of surface Kondo effect discussed above. Tilting the field out of plane, $\rho(\theta = 90)$ is found to be rather complicated,

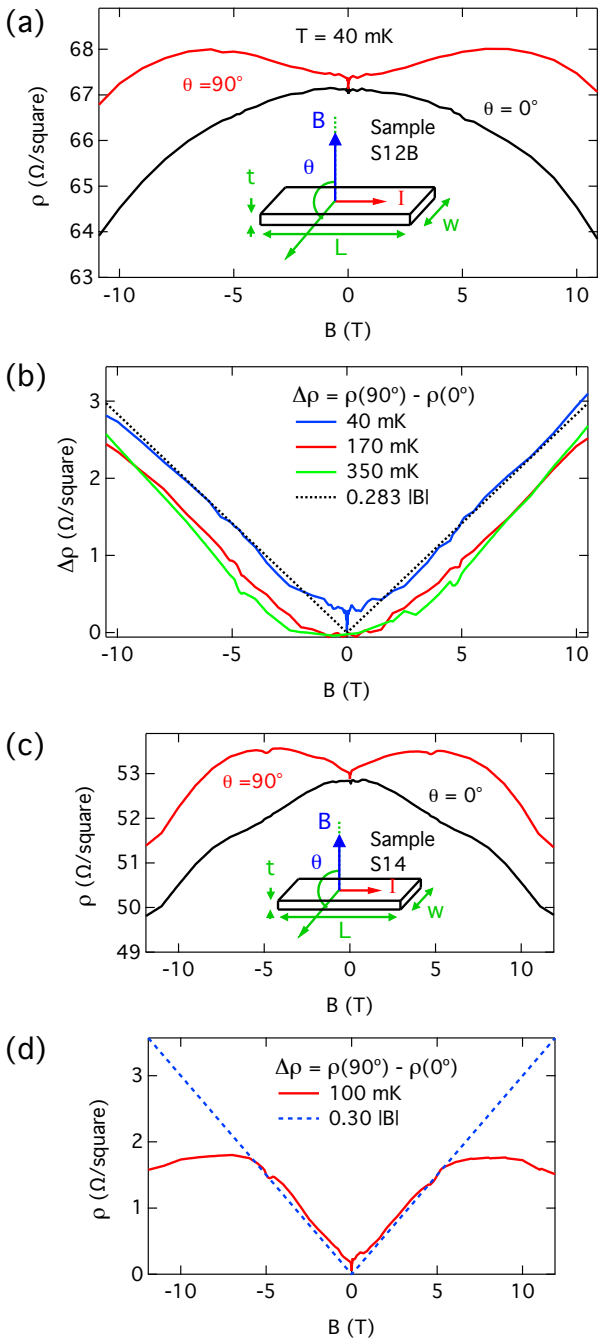

FIG. 5: **Linear magnetoresistance**. **(a)**, Magnetoresistance (MR) of sample S12B with perpendicular and in-plane magnetic fields at 40 mK. The zero field dip in $\rho(90^\circ)$ is due to WAL effect. **(b)**, Above 1 Tesla, orbital MR $\Delta\rho = \rho(90^\circ) - \rho(0^\circ)$ shows linear field dependence. **(c, d)**, MR of sample S14 at 100 mK, showing that the orbital part of MR is linear with magnetic field below 5 Tesla.

but we can extract the orbital contribution to the MR using $\Delta\rho = \rho(\theta = 90^\circ) - \rho(\theta = 0^\circ)$. As shown in Fig. 5b, apart from the sharp dip near zero field due to WAL, $\Delta\rho$ is positive and linear for $B > 1\ T$. The linearity doesn't seem to change when temperature is raised to 350 mK. Linear MR is known to occur in metals with an open Fermi surface[22], which is not the case for SmB_6 according to recent ARPES results[8–10]. Disorder or geometry effects could also give rise to linear MR due to symmetric mixing of Hall voltages[23]. However, in our sample the magnetoresistance $\Delta R_{xx} = \Delta\rho\ L/w$ is 3 times larger than the Hall resistance R_{xy} and makes this scenario unlikely. The electric contacts were made via spot welding with less than 5 Ω contact resistance, which is significantly smaller than the sample resistance. Interestingly, linear and temperature-independent MR is predicted[24] to occur in zero-gap materials with Dirac dispersion in the quantum limit of a few Landau levels, and is indeed found in Bi-based topological insulators (a review see[25]) and in graphene[26]. In SmB_6 recent surface quantum oscillation experiment[11] has identified a relatively large surface carrier density and quite a few Landau levels are occupied for the α pocket at 10-Tesla magnetic field. This is not the single Landau level scenario considered in the theory[24], therefore further theoretical calculations or other scenarios are required to explain the linear MR discovered here.

In conclusion, we have verified the existence of a conductive surface of SmB_6 down to 20 mK without signs of localization. The observed WAL effect on the SmB_6 surface state is consistent with the picture of a TSS with spin-momentum-locking. The saturation of the surface resistivity follows a logarithmic temperature dependence that could be explained by Kondo effect due to the interaction between the surface state and a Kondo lattice with unavoidable defects. In addition, a proper description of the SS of SmB_6 needs to be consistent with the observed magnetoresistance that contains a negative Zeeman term and a positive linear orbital term.

Acknowledgements: This work is supported by NSF grant DMR-1350122. Stimulating discussions with V. Galitski, R. Greene, C. Kurdak and M. Dzero are greatly appreciated.

[1] Z. Fisk, J.L. Sarrao, J.D. Thompson, D. Mandrus, M.F. Hundley, A. Miglori, B. Bucher, Z. Schlesinger, G. Aeppli, E. Bucher, J.F. DiTusa, C.S. Oglesby, H-R. Ott, P.C. Can-

field, S.E. Brown,, Kondo insulators, Physica B 223-224, 409-412 (1996).

[2] A. Menth, E. Buehler, T. Geballe, Magnetic and Semiconducting Properties of SmB_6, Phys Rev Lett 22, 295-297 (1969).

[3] M. Dzero, K. Sun, V. Galitski, P. Coleman. Topological Kondo Insulators, Phys Rev Lett 104, 106408 (2010).

[4] S. Wolgast, C. Kurdak, K. Sun, J. W. Allen, D. Kim, Z. Fisk, Low-temperature surface conduction in the Kondo insulator SmB_6, Phys. Rev. B 88, 180405(R) (2013).

[5] X. Zhang, N. P. Butch, P. Syers, S. Ziemak, R. L. Greene, J. Paglione, Hybridization, Inter-Ion Correlation, and Surface States in the Kondo Insulator SmB_6, Phys. Rev. X 3, 011011 (2013).

[6] D. J. Kim, S. Thomas, T. Grant, J. Botimer, Z. Fisk, Jing Xia, Surface Hall Effect and Nonlocal Transport in SmB_6: Evidence for Surface Conduction, Scientific Reports 3, 3150 (2013).

[7] D. J. Kim, J. Xia, Z. Fisk, Topological surface state in the Kondo Insulator Samarium Hexaboride, Nature Materials, 13, 446-470 (2014).

[8] M. Neupane, N. Alidoust, S-Y. Xu, T. Kondo, Y. Ishida, D. J. Kim, Chang Liu, I. Belopolski, Y. J. Jo, T-R. Chang, H-T. Jeng, T. Durakiewicz, L. Balicas, H. Lin, A. Bansil, S. Shin, Z. Fisk, M. Z. Hasan, Surface electronic structure of the topological Kondo-insulator candidate correlated electron system SmB6, Nature Communications 4, 2991 (2013).

[9] N. Xu, X. Shi, P. K. Biswas, C. E. Matt, R. S. Dhaka, Y. Huang, N. C. Plumb, M. Radovic, J. H. Dil, E. Pomjakushina, K. Conder, A. Amato, Z. Salman, D. McK. Paul, J. Mesot, H. Ding, M. Shi, Surface and Bulk Electronic Structure of the Strongly Correlated System SmB_6 and Implications for a Topological Kondo Insulator, Phys. Rev. B 88, 121102(R) (2013).

[10] J. Jiang, S. Li, T. Zhang, Z. Sun, F. Chen, Z.R. Ye, M. Xu, Q.Q. Ge, S.Y. Tan, X.H. Niu, M. Xia, B.P. Xie, Y.F. Li, X.H. Chen, H.H. Wen, D.L. Feng, Observation of possible topological in-gap surface states in the Kondo insulator SmB6 by photoemission, Nature Communications 4, 3010 (2013).

[11] G. Li, Z. Xiang, F. Yu, T. Asaba, B. Lawson, P. Cai, C. Tinsman, A. Berkley, S. Wolgast, Y. S. Eo, Dae-Jeong Kim, C. Kurdak, J. W. Allen, K. Sun, X. H. Chen, Y. Y. Wang, Z. Fisk, Lu Li, Two-dimensional Fermi surfaces in Kondo insulator SmB_6, Science 346, 6214, 1208 (2013).

[12] V. Alexandrov, M. Dzero, P. Coleman, Cubic Topological Kondo Insulators, Phys Rev Lett 111, 226403 (2013).

[13] F. Lu, J. Zhao, H. Weng, Z. Fang, X. Dai, Correlated Topological Insulators with Mixed Valence, Phys Rev Lett 110, 096401 (2013).

[14] X.-L. Qi, S.-C. Zhang, Topological insulators and superconductors, Rev Mod Phys 83, 1057-1110 (2011).

[15] M. Hasan, C. Kane, Colloquium: Topological insulators, Rev Mod Phys 82, 3045-3067 (2010).

[16] B. L. Altshuler, A. A, Electron-electron Interactions In Disordered Conductors (Elsevier, New York, ed. 1, 1985), pp. 1-159.

[17] S. Hikami, A. I. Larkin, Y. Nagaoka, Spin-Orbit Interaction and Magnetoresistance in the Two Dimensional Random System, Prog. Theor. Phys. 63, 707710 (1980).

[18] M. Dzero, K. Sun, P. Coleman, V. Galitski, Theory of topological Kondo insulators, Phys Rev B 85, 045130 (2012).

[19] J. Kondo, Resistance Minimum in Dilute Magnetic Alloys, Prog. Theor. Phys. 32, 37-49 (1964).

[20] T. A. Costi, A. C. Hewson, V. Zlatic, Transport-Coefficients of the Anderson Model via the Numerical Renormalization-Group, J Phys-Condens Mat 6, 2519-2558 (1994).

[21] J. C. Cooley et al., High Field Gap Closure in the Kondo Insulator SmB_6, Journal of Superconductivity 12, 171-173 (1999).

[22] P. Kapitza, The Study of the Specific Resistance of Bismuth Crystals and Its Change in Strong Magnetic Fields and Some Allied Problems, Proceedings of the Royal Society of London 119, 358 (1928).

[23] M. M. Parish, P. B. Littlewood, Non-saturating magnetoresistance in heavily disordered semiconductors, Nature 426, 162-165 (2003).

[24] A. A. Abrikosov, Quantum magnetoresistance, Phys Rev B 58, 2788 (1998).

[25] M. Veldhorst, M. Snelder, M. Hoek, C. G. Molenaar, D. P. Leusink, A. A. Golubov, H. Hilgenkamp, A. Brinkman, Magnetotransport and induced superconductivity in Bi based three-dimensional topological insulators, Physica Status Solidi-Rapid Research Letters 7, 26-38 (2013).

[26] Adam L. Friedman, Joseph L. Tedesco, Paul M. Campbell, James C. Culbertson, Edward Aifer, F. Keith Perkins, Rachael L. Myers-Ward, Jennifer K. Hite, Charles R. Eddy, Glenn G. Jernigan, D. Kurt Gaskill, Quantum linear magnetoresistance in multilayer epitaxial graphene, Nano Lett 10, 3962-3965 (2010).

[27] M. Dzero, M. G. Vavilov, K. Kechedzhi, and V. M. Galitski, Phys. Rev. B 92, 165415 (2015)